

Estimating oceanic primary production using vertical irradiance and chlorophyll profiles from ocean gliders in the North Atlantic

Victoria S. Hemsley^{1,2}, Timothy J. Smyth³, Adrian P. Martin², Eleanor Frajka-Williams¹,
Andrew F. Thompson⁴ Gillian Damerell⁵ and Stuart C. Painter²*

¹ University of Southampton, National Oceanography Centre, European Way, Southampton,
SO14 3ZH, UK

² National Oceanography Centre, Southampton, SO14 3ZH, UK

³ Plymouth Marine Laboratory, Prospect Place, The Hoe, Plymouth, PL1 3DH, UK

⁴ Environmental Science & Engineering, California Institute of Technology, Pasadena, US

⁵ School of Environmental Sciences, University of East Anglia, Norwich, UK

Contact details

Victoria Hemsley

vsh1g12@soton.ac.uk

Supporting Information

Pages: 9

Figures: 6

Tables: 0

Satellite Chlorophyll Profiles

The satellite chlorophyll (c) was used to calculate full depth profiles using relationships derived by Morel and Berthon relating satellite chlorophyll to the shape of the profile at depth.¹⁴ A Gaussian curve, with a maximum value (C_{max}) situated at (ζ_{max}) and a thickness controlled by ($\Delta\zeta$), is fitted over a background (C_b), Equations are shown below:

$$\frac{C(\zeta)}{\bar{C}_{ze}} = C_b + C_{max} \exp \left\{ - \left[\frac{\zeta - \zeta_{max}}{\Delta\zeta} \right]^2 \right\},$$

with

$$C_b = 0.768 + 0.087 \log c - 0.179(\log c)^2 - 0.025(\log c)^3$$

$$C_{max} = 0.299 - 0.289 \log c + 0.579 (\log c)^2$$

$$\zeta_{max} = 0.600 - 0.640 \log c + 0.021(\log c)^2 + 0.115(\log c)^3$$

and

$$\Delta\zeta = 0.710 + 0.159 \log c + 0.021(\log c)^2.$$

Where $C(\zeta)/\bar{C}_{ze}$ is normalised chlorophyll; chlorophyll divided by the mean pigment concentration in the euphotic layer, where $\bar{C}_{ze} = 1.12 c^{0.803}$. The full methods are described in Morel and Berthon.¹⁴

Fluorescence Quenching

We obtained a linear regression between 132 night-time profiles of chlorophyll and backscatter counts to a depth of 60 m. This regression, represented by the equation chlorophyll concentration = 0.0455 * backscatter - 3.2 (Spearman⁵⁵ $R^2 = 0.87$, $p < 0.001$, $n = 132$) was used to correct daytime chlorophyll profiles affected by quenching. Due to the

dominance of diatoms in the pre-bloom phytoplankton community structure,²⁶⁻²⁹ to our knowledge diel vertical migration should not impact heavily on the quenching corrections.

When a subsurface chlorophyll maxima (SCM) was present the night-time relationship between optical backscatter and chlorophyll weakened, with R^2 values reducing from ~ 0.87 to ~ 0.64 . The decision was made not to correct for quenching when an SCM was present for two reasons: firstly surface chlorophyll concentrations were substantially lower when a SCM was present and there was little difference in surface and SCM chlorophyll concentrations between night and day profiles ($< 5\%$). In late spring the mean difference in surface chlorophyll concentrations between night and day profiles was $2.1 \text{ mg chl m}^{-3}$. However when a persistent SCM was present the mean difference in surface chlorophyll concentrations was $< 0.2 \text{ mg chl m}^{-3}$.

Validation of glider PAR

Although absolute PAR values are not needed to calibrate chlorophyll fluorescence they are needed for input into the primary production algorithm. Validating the glider PAR instrument on the Seaglider was done with a linear least squares regression between the ship and glider surface PAR. All observations were coincident to within 100 km, a distance over which we expect any minor differences in irradiance to be due to significant differences in cloud cover and/or type, assuming identical sun angle and intensity. Ship-based PAR data were extracted within one minute of each glider surfacing and the resultant time series correlated to $I(0^+)$ estimates from the glider (Eq. 2). The resulting correlation was significant (Spearman's⁵⁵ $R^2 = 0.48$, $p < 0.005$, $n = 83$) but revealed substantial variation between ship-based and glider-based measurements particularly at midday. The standard deviation of differences over 10 minutes of the measurement was calculated for the ship-based PAR; reaching up to 100 W m^{-2}

², with a mean standard error of $\pm 14 \text{ W m}^{-2}$. This is likely due to patchy cloud cover shading the ship. The coefficient of variation was generally less than 0.6 suggesting a high variance. Errors increased late in the evening and early morning when PAR values are very low and sensor geometry can play a significant role.

To evaluate the strength of the linear regression between glider and ship PAR a bootstrapping method was applied, we randomly selected 90% of the data points, 10,000 times, and calculated the regression for each subset. The distribution of the slopes was normal with a mean of 0.96 and a standard deviation of 0.076. We concluded that the true slope and intercept were indistinguishable from one and zero. Based on this analysis, glider and shipped-based PAR estimates agree so the glider PAR data were used with the manufacturer's calibration applied.

Calculating sea surface reflectance

Fresnel reflectance estimates the reflectance of light on a flat water surface when moving between media of different refractive indices, such as air and water, and is determined from the angle of the incident light. The direct and diffuse irradiance was calculated as described by Mobley⁴³. The Fresnel reflectance (r) was computed from the solar zenith angle (θ) as described by Kirk⁴⁴ (Eq.1)

$$r = 0.5 \frac{\sin^2(\theta_a - \theta_w)}{\sin^2(\theta_a + \theta_w)} + 0.5 \frac{\tan^2(\theta_a - \theta_w)}{\tan^2(\theta_a + \theta_w)} \quad [\text{S1}]$$

where θ_a is the zenith angle of the incident light in air, and θ_w the angle to the downward vertical of the transmitted beam in water. The angle θ_w is determined by θ_a and the refractive index for water and air (n_w , n_a , respectively) as

$$\frac{\sin \theta_a}{\sin \theta_w} = \frac{n_w}{n_a}. \quad [\text{S2}]$$

To estimate the reflectance of water more accurately, as it is not always a homogenous surface assumed by the Fresnel equation, the effect of foam (r_f) was calculated from the wind speed (ws)⁴³ (HYDROLIGHT). Foam increases the reflectivity of the water surface, allowing diffuse and direct irradiance to be estimated, which are used for calculating the total reflectance.⁷⁷ When the wind speed (<http://www.ecmwf.int/>) was less than 7 m s⁻¹ the following equation was used to calculate the fraction of the surface covered with foam (cn),

$$cn = \frac{6.2 \times 10^{-4} + 1.56 \times 10^{-3}}{ws}, \quad [S3a]$$

where the effect of foam is

$$r_f = \rho_a cn 2.2 \times 10^{-5} ws^2 - 4.0 \times 10^{-4}. \quad [S4a]$$

where ρ_a is the density of air (1.2×10^{-3} g m⁻³). If the wind speed was greater than 7 m s⁻¹ we used modified equations

$$cn = 0.49 \times 10^{-3} + 0.065 \times 10^{-3} ws, \quad [S3b]$$

$$r_f = (\rho_a cn 4.5 \times 10^{-5} - 4.0 \times 10^{-5}) ws^2 \quad [S4b]$$

The direct light reflectance term (r_d) represents the light reflected in one direction only. This increases with increasing sun angle, and can be calculated from the foam reflectance together with the Fresnel reflectance (r)

$$r_d = r_f + r. \quad [S5]$$

The diffuse reflectance term (r_{diff}), which represents the reflectance of light in all directions, was set to a value of 0.066 if the foam reflectance was equal to zero. However, when r_f was greater than zero r_{diff} was calculated as:

$$r_{diff} = r_f + 0.057. \quad [S6]$$

Parameterisations of Net growth rate (a^*) and Absorption cross section

These values are parameterised as in Morel et al. (1996),⁵⁴ where a^* is 0.033 m^{-1} .

Temperature from the glider CTD is used to parameterise ϕ_μ using the following equations:⁴²

$$\begin{aligned}\phi_\mu &= \phi_{\mu\max} f(x), \\ f(x) &= x^{-1}(1 - e^{-x})e^{-\beta x}, \\ x &= PUR/KPUR\end{aligned}$$

and

$$\phi_\mu KPUR(T) = KPUR(20^0)1.065^{(T-20^0)},$$

where $\phi_{\mu\max}$ is set to $0.06 \text{ mol C (mol quanta)}^{-1}$ and $f(x)$ is formulated according to the photosynthesis-irradiance curve (Platt 1980). β is a unitless photoinhibition parameter set to 0.01. PUR is the Photosynthetic Useful Radiation (PAR weighted by chlorophyll-a specific absorption spectrum and $KPUR$ is derived from temperature (T), which is provided by the glider PAR sensor (Section 3.1.3.)).

Figure S1

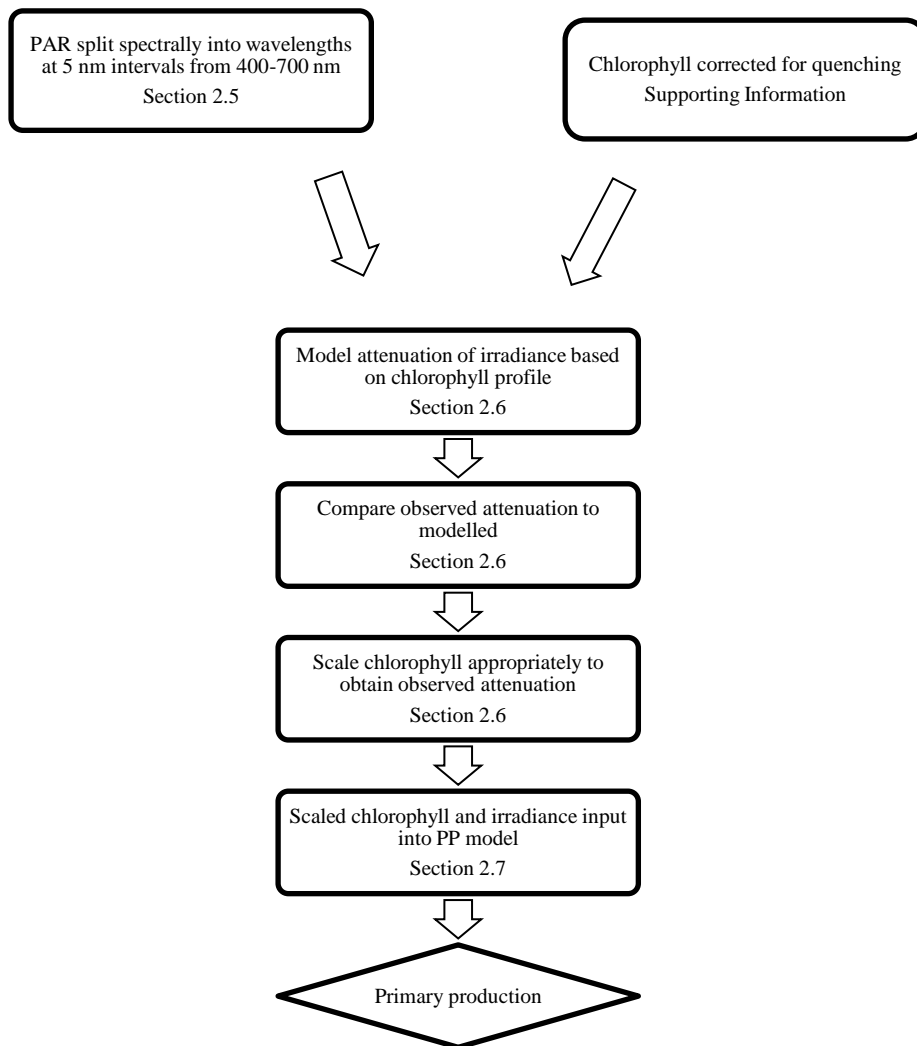


Figure S1: Flow diagram explaining the steps needed to be taken to calibrate and subsequently calculate primary production from a glider.

Figure S2

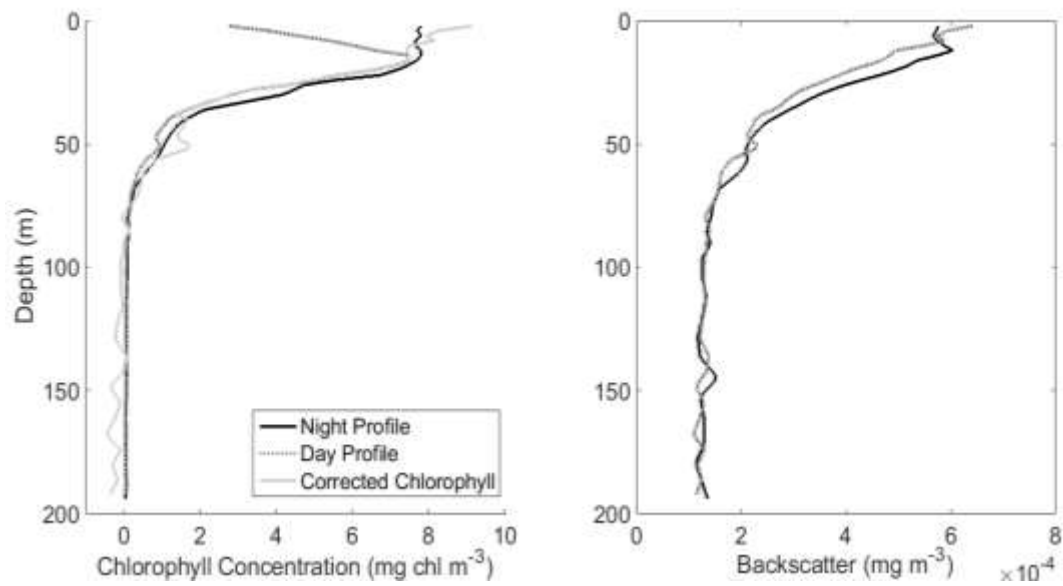


Figure S2: Chlorophyll and backscatter day and night profiles. The chlorophyll profile during the day is noticeably lower in the surface. Suggests that the extent of quenching is to a depth of 20m. The resulting corrected chlorophyll is also plotted.

Figure S3

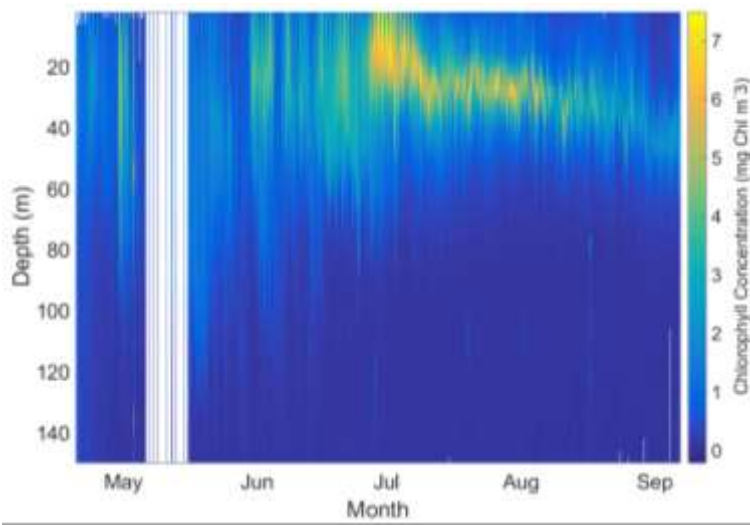


Figure S3: Original chlorophyll profiles observed from Seaglider, with manufactures' calibration only. Note the daily depression in the surface chlorophyll due to quenching and high chlorophyll values $> 7 \text{ mg Chl m}^{-3}$.

Figure S4

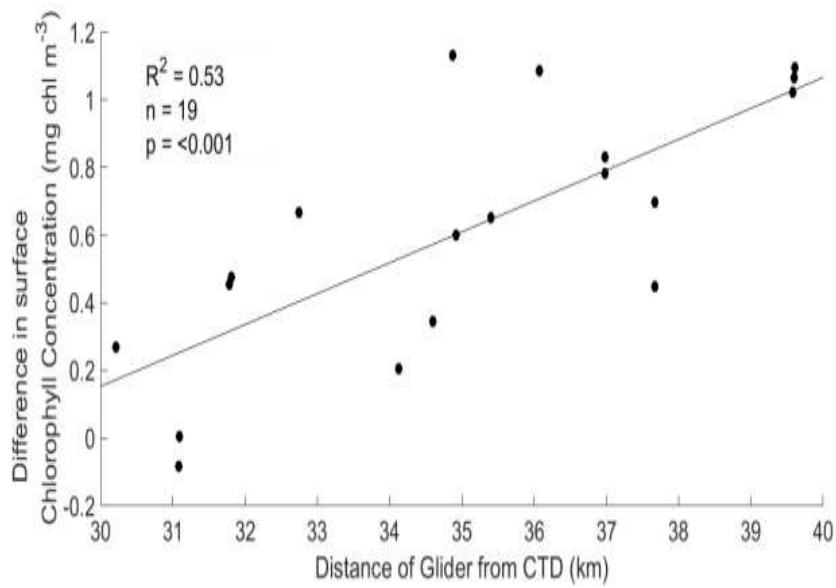


Figure S4: Distance of glider to CTD casts compared with difference in surface chlorophyll concentrations from the glider or the cast. Regression is significant ($R^2 = 0.53$, $n = 19$, $p = <0.001$).

Figure S5

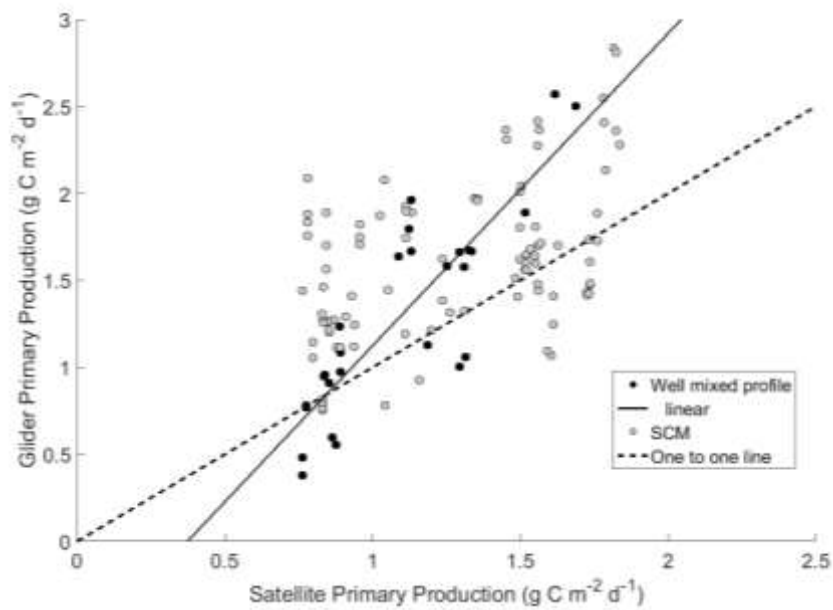


Figure S5: Relationship between PP estimates using NEODAAS 1km daily satellite chlorophyll and estimates calculated for SG566. Regression line calculated as a reduced major axis regression. Filled black dots show well-mixed chlorophyll profiles, filled grey dots show chlorophyll profile after year day 180 when an SCM formed and the satellite chlorophyll profile was estimated from Morel and Berthon.⁴²

Figure S6

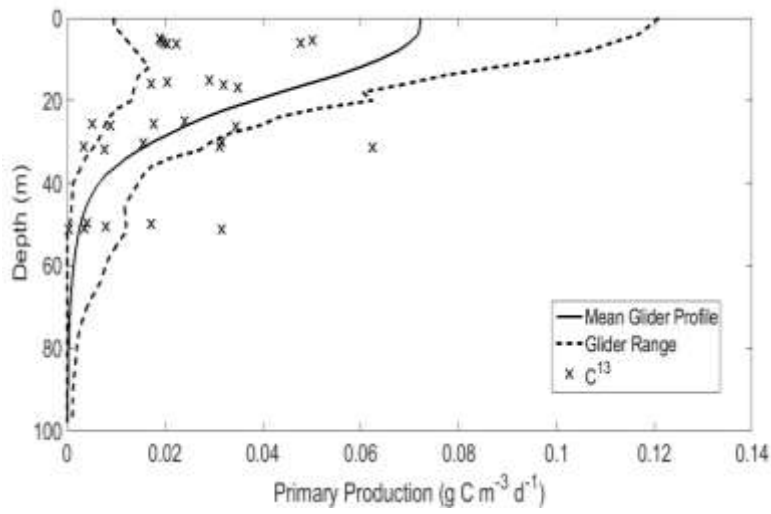


Figure S6: Depth profiles of CTD ¹³C measurements, alongside glider estimated depth profiles, with a median profile for the duration of the ¹³C measurements and the range of the estimated glider profiles.